Wave, Boy's Surface, and Machine

Annie Wei[1] and Yongheng Zhang[2]

Department of Mathematics and Statistics, Amherst College, MA, USA
[1]arwei25@amherst.edu, [2]yzhang@amherst.edu

Abstract

We describe an analytical method of constructing Boy's surface which uses Thurston's corrugation technique to add period-3 waves to an image of the 2-sphere. This construction allows us to build a simple machine which can draw Boy's surface in space.

Introduction

A hundred and twenty-two years ago, David Hilbert suspected that it is impossible to immerse the real projective plane $\mathbb{R}P^2$ in $\mathbb{R}^3$. He asked his doctoral student Werner Boy to prove it. Instead, Boy discovered the opposite, finding an immersed image of $\mathbb{R}P^2$, later called Boy's surface. Boy's description was qualitative, relying mostly on pictures. Afterwards, analytical formulas were found, such as those by Morin, Petit-Souriau, Hughes, Bryant-Kusner, and Apéry, summarized in the book [1]. In this paper, we present another analytical formula, which inspired the construction of a simple machine that draws Boy's surface in space.

To understand the abstract surface $\mathbb{R}P^2$, imagine the planet Earth, modeled by the unit sphere S^2 in $\mathbb{R}^3$, with the north pole N at $(0, 0, 1)$ and the south pole S at $(0, 0, -1)$. On $\mathbb{R}P^2$, these two poles are considered the same point, and in general, $\mathbb{R}P^2$ identifies any two antipodal points on S^2. It is not immediately clear that $\mathbb{R}P^2$, an abstract geometric space, can be immersed in $\mathbb{R}^3$, as its representation would possess qualities which are difficult to visualize. For example, unlike S^2, $\mathbb{R}P^2$ contains a Möbius strip, so it must intersect itself as a closed surface in $\mathbb{R}^3$ [8]. Additionally, the surface must contain a triple point [2].

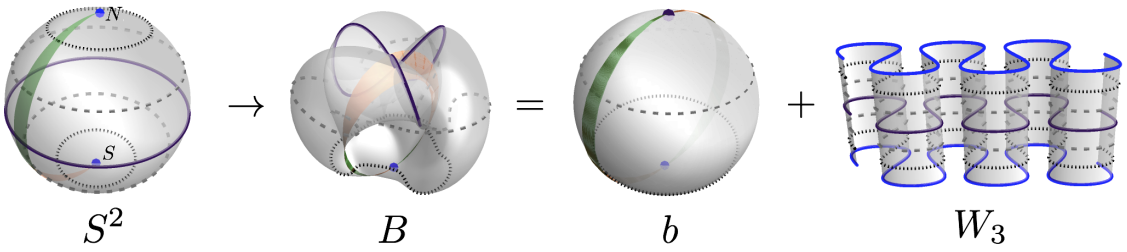

Figure 1: *Boy's surface is an image of S^2 in $\mathbb{R}^3$; The formula $B = b + W_3$.*

The Boy's surface constructed in this paper is an immersed image of a smooth map $B : S^2 \to \mathbb{R}^3$ with each pair of antipodal points mapped to the same location. B is given by the formula

$$B = b + W_3, \tag{1}$$

where $b : S^2 \to \mathbb{R}^3$ is a base map collapsing the equator to a single point, and is thus not an immersion. To remove this singularity without creating new singularities, we add $W_3 : S^2 \to \mathbb{R}^3$, a period-3 wavy surface which wraps around the image of b via an orthonormal frame field, and whose amplitude grows from zero at the poles to a maximum on the equator. This method of viewing a surface as the composition of a simpler

base surface and a wavy surface (Figure 1) is due to William Thurston. It was used in his method of everting the sphere, as illustrated in the movie *Outside In* [6].

In this paper, we first review the analytical theory of Thurston's corrugation method [7] using curves in the plane, as an analogy for understanding the subsequent 3D construction of the Boy's surface. Then we describe a machine inspired by Formula (1), which is used to paint Boy's surface in the dark using electronic lights.

Wave

Consider the parametrized curve $f(t) = \langle y(t), z(t) \rangle$ on the yz plane:

$$y(t) = \begin{cases} -2\cos 2t & 0 \le t \le \pi/2 \\ 2 & \pi/2 < t \le \pi \\ 2\cos 2t & \pi < t \le 3\pi/2 \\ -2 & 3\pi/2 < t \le 2\pi \end{cases} \qquad z(t) = \begin{cases} 1 & 0 \le t \le \pi/2 \\ -\cos 2t & \pi/2 < t \le \pi \\ -1 & \pi < t \le 3\pi/2 \\ \cos 2t & 3\pi/2 < t \le 2\pi \end{cases}$$

(a) *The components $y(t)$ and $z(t)$ are C^1.* **(b)** *But $f'(t) = \langle 0, 0 \rangle$ at the four vertices.*

Figure 2: *The rectangular curve $f(t) = \langle y(t), z(t) \rangle$ is C^1 but not regular.*

The curve f is C^1, as both derivatives $y'(t)$ and $z'(t)$ exist and are continuous (Figure 2a). However, f is not regular as f' vanishes at four points. Its image is a rectangle, with four sharp corners (singularities) at points where $f'(t) = \langle 0, 0 \rangle$ (Figure 2b). We will remove the singularities of f by adding waves, which we construct using the following periodic curve $\mathbf{8} : \mathbb{R} \to \mathbb{R}^2$:

$$\mathbf{8}(t) = \langle -\sin 2t, 2\sin t \rangle.$$

As t increases from 0 to 2π, $\mathbf{8}$ begins at the origin, moves northwest, then traces an "8" on the yz plane (Figure 3a). The derivative $\mathbf{8}'$ lies in an annular sector missing the quarter symmetric about the negative y-axis (Figure 3b). This feature is important for maintaining regularity when the amplitude of waves become variable and small, especially near the poles of the base map b in Formula (1) as we'll see in the next section.

Now consider $a\mathbf{8}(nt)$, which is $\mathbf{8}$ with adjusted amplitude a and frequency n of oscillation. Adding to $f(t)$ gives:

$$F_1(t) = f(t) + a\mathbf{8}(nt),$$

shown in Figure 4a. To see that $F_1(t)$ is regular, note $f'(t)$ is continuous over the compact domain $[0, 2\pi]$, so $f'(t)$ is bounded, and we may choose a and n such that an large causes $an\mathbf{8}'(nt)$ to lie outside a sufficiently big circle containing $f'(t)$ in its interior. This ensures $\left|an\mathbf{8}'(nt)\right| > \left|f'(t)\right|$ everywhere, which implies that $F_1'(t)$ is never zero. For F_1 to keep semblance with f, the amplitude a of the waves cannot be too large, but this is compensated with big n. Note that adding $\mathbf{8}$ may change a curve from an embedding to an immersion, as is the case for F_1.

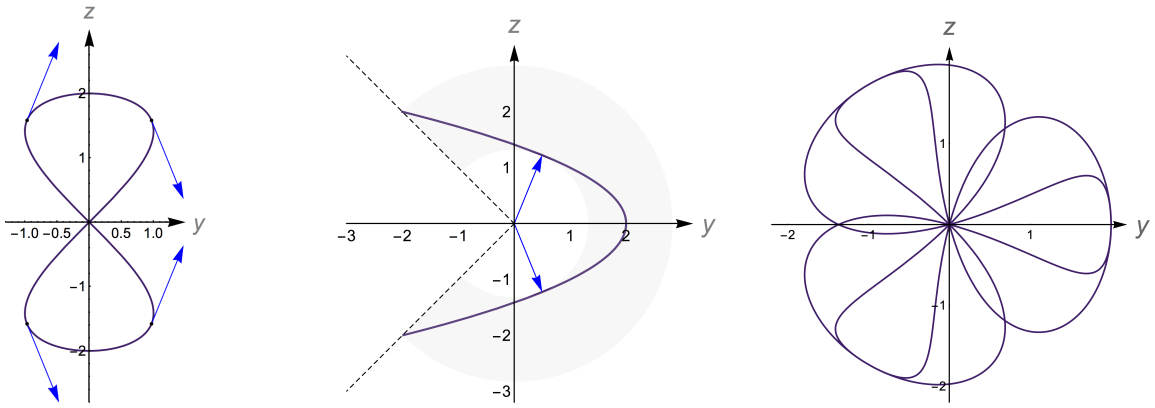

(a) *Image of* $\mathbf{8}$. **(b)** *Image of* $\mathbf{8}'$. **(c)** $G(t) = g(t) + R(t)\mathbf{8}(3t)$.

Figure 3: *The model figure-8 curve and its derivative used in this paper; Planar "trefoil".*

When constructing the 3D Boy's surface, pointwise variation of amplitude and pointwise rotation of waves are also necessary. In the 2D case, the former can be done using a C^1 function $A(t)$:

$$F_2(t) = f(t) + aA(t)\mathbf{8}(nt),$$

which is illustrated in Figure 4b with $A(t) = 1 + 1/2\cos 4t$. The latter can be done using a C^1 map $R : \mathbb{R} \to SO(2)$, where $SO(2)$ is the space of 2×2 orthonormal matrices with determinant 1:

$$F_3(t) = f(t) + aA(t)R(t)\mathbf{8}(nt).$$

The result of pointwise rotation is shown in Figure 4c with $R(t) = \begin{bmatrix} \cos t & -\sin t \\ \sin t & \cos t \end{bmatrix}$.

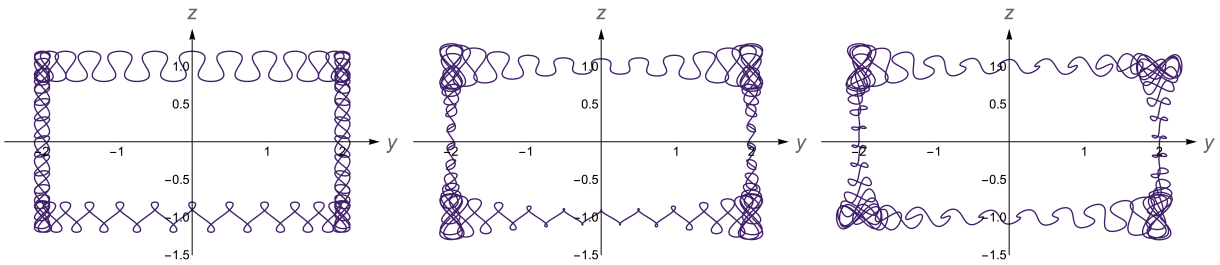

(a) $F_1(t) = f(t) + a\mathbf{8}(nt)$. **(b)** $F_2(t) = f(t) + aA(t)\mathbf{8}(nt)$. **(c)** $F_3(t) = f(t) + aA(t)R(t)\mathbf{8}(nt)$.

Figure 4: *Corrugated rectangles where* $a = 0.1$ *and* $n = 50$.

The formula for Boy's surface to be discussed in the next section is a 3D version of $F_3(t)$ using corrugation with much lower frequency ($n = 3$). The corrugation, whose waves expand and rotate in 3D space, is used to remove a singularity that is the image of the equator. Its effect can be understood by the 2D example in Figure 3c where $g(t) := \langle 0, 0 \rangle$ maps a circle to a single point, and is thus not regular. The addition of $R(t)\mathbf{8}(3t)$ introduces three uniformly rotated "8"s to g so that G is regular, and whose corrugation is contained to the plane. In 3D, the extra dimension provides space where the image of the equator can be folded into a twice traversed trefoil.

Boy's Surface

Consider the sphere S^2 as our planet Earth and let ϕ be the polar angle, i.e., the angle of latitude, which is $\pi/2$, 0 and $-\pi/2$, at the north pole, the equator and the south pole, respectively. Let θ be the azimuthal angle, i.e., the angle of longitude, which is 0 for the prime meridian (the half circle from pole to pole intersecting the positive x-axis), and is the same θ as in spherical coordinates. The definition of ϕ differs from spherical coordinates, as rather than measured from the positive z-axis downward, it is measured from the xy-plane upward as shown in Figure 5a.

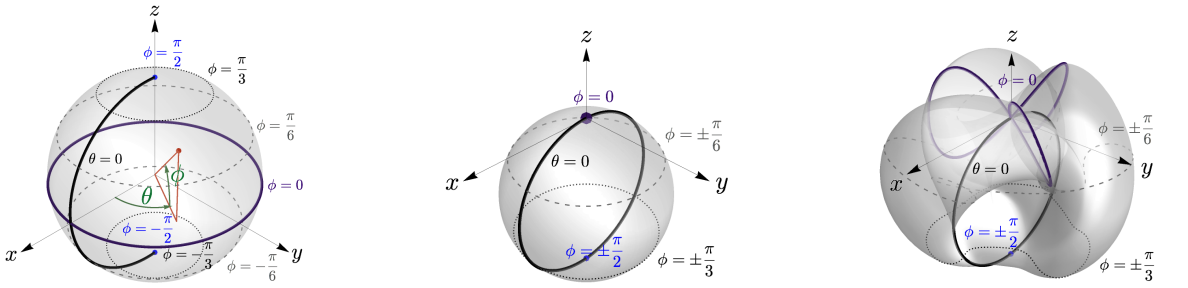

(a) *Definition of θ and ϕ.* **(b)** *Image of b* **(c)** *Image of B*

Figure 5: *The sphere S^2, the image of the base map b, and the Boy's surface in this paper.*

Define the base map $b : S^2 \to \mathbb{R}^3$ as:

$$b(\theta, \phi) = r(\theta)l(\phi),$$

where $r(\theta)$ is the rotation matrix about the z-axis through angle θ, i.e. $r(\theta) = \begin{bmatrix} \cos\theta & -\sin\theta & 0 \\ \sin\theta & \cos\theta & 0 \\ 0 & 0 & 1 \end{bmatrix}$, and $l(\phi) = \langle 0, 0, -\frac{1}{2}\rangle + \frac{1}{2}\langle -\sin 2\phi, 0, \cos 2\phi\rangle$, with "$\langle$" and "$\rangle$" enclosing column vectors. The image of b is shown in Figure 5b with θ and ϕ values.

One can check that $b(\theta + \pi, -\phi) = b(\theta, \phi)$, so b maps antipodal points on S^2 to the same point in $\mathbb{R}^3$. Thus, the image of b is a representation of $\mathbb{R}P^2$ in $\mathbb{R}^3$. Note b is regular[1] everywhere except on the equator $\phi = 0$, which is mapped to a single point by b. To remove this singularity, we add waves to the base map b.

Let $\mathbf{8} : \mathbb{R} \to \mathbb{R}^3$ be defined by $\mathbf{8}(t) = \langle 0, -\sin 2t, 2\sin t\rangle$. This is the $\mathbf{8}$ in the previous section as a spatial curve, and we add it to b after adjusting its orientation, amplitude, and period.

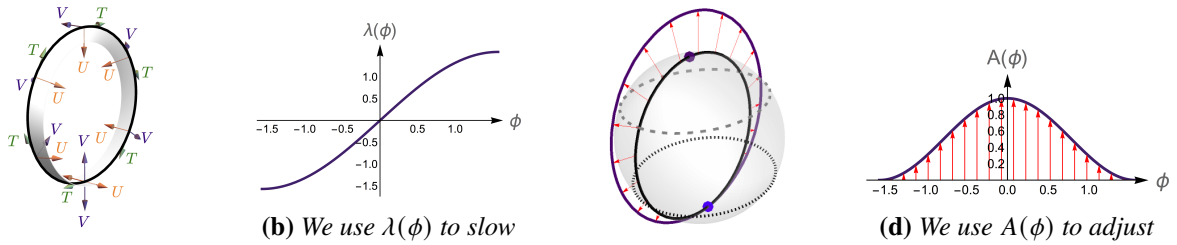

(a) *Orthonormal frames along $l(\phi)$.* **(b)** *We use $\lambda(\phi)$ to slow down the turning of frames near the poles.* **(c)** *The amplitude $aA(\phi)$ seen on $l(\phi)$.* **(d)** *We use $A(\phi)$ to adjust the amplitude of waves, which is 0 at the poles.*

Figure 6: *The frame $R(\phi)$, the saturation function $\lambda(\phi)$ and the amplitude adjusting function $A(\phi)$.*

An orthonormal frame field $R(\phi) = \big[T(\phi), U(\phi), V(\phi)\big]$, pictured in Figure 6a, rotates $\mathbf{8}$. The columns of $R(\phi)$ are defined as follows.

[1]That b is regular means away from the poles, $\frac{\partial b}{\partial \phi}$ and $\frac{\partial b}{\partial \theta}$ are linearly independent; in neighborhoods at the poles, we can use Cartesian coordinates: $\frac{\partial b}{\partial x}$ and $\frac{\partial b}{\partial y}$ are linearly independent. On the equator $\phi = 0$, $\frac{\partial b}{\partial \theta} = \langle 0, 0, 0\rangle$ so b is not regular.

First, $T(\phi) := l'(\phi)$ or the unit tangent vector along the image of the prime meridian:

$$T(\phi) = \langle -\cos 2\phi, 0, -\sin 2\phi \rangle.$$

Second, $U(\phi)$ is a vector turning about $T(\phi)$, which we define using $N(\phi)$, a unit vector perpendicular to $T(\phi)$ that points toward $(0, 0, -1/2)$, the center of the image of b:

$$N(\phi) = \langle \sin 2\phi, 0, -\cos 2\phi \rangle.$$

Then $U(\phi)$ is a vector turning about $T(\phi)$ on the plane spanned by $\langle 0, 1, 0 \rangle$ and $N(\phi)$. As ϕ goes from $-\pi/2$ to $\pi/2$, $U(\phi)$ completes a half twist from $\langle 0, 1, 0 \rangle$ to $\langle 0, -1, 0 \rangle$ through angle π. We also use $\lambda(\phi) = \frac{\pi}{2}\sin(\phi)$ to slow down the turning of $U(\phi)$ near the poles (Figure 6b). Altogether, $U(\phi) = -\sin\lambda(\phi)\langle 0, 1, 0 \rangle + \cos\lambda(\phi)N(\phi)$, or:

$$U(\phi) = \langle \cos\lambda(\phi)\sin 2\phi, -\sin\lambda(\phi), -\cos\lambda(\phi)\cos 2\phi \rangle.$$

Lastly, $V(\phi) := T(\phi) \times U(\phi)$ completes the frame:

$$V(\phi) = \langle -\sin\lambda(\phi)\sin 2\phi, -\cos\lambda(\phi), \sin\lambda(\phi)\cos 2\phi \rangle.$$

We can think of $R(\phi)$ as a miniature coordinate system, in which **8** is traced, oriented differently from point to point on the image of l. $R(\phi)$ is an element of $SO(3)$, the space of orthonormal matrices with determinant 1.

At the moment, there is an ambiguity of $R(\phi)$ at the poles after applying $r(\theta)$, as $r(\theta)R(\pm\frac{\pi}{2})$ is different for different θ. To remedy this, we annihilate **8** at the poles using the C^1 function $A(\phi) = \frac{1}{2} + \frac{1}{2}\cos 2\phi$. In Figure 6d we see $A(\phi)$ grows from zero at the poles of S^2 (with derivative zero) to a maximum value on the equator. Figure 6c shows the resulting change in the image. The maximum amplitude a is set to be 0.25 in Figures 1, 5c, 7b, and the second row of 8, though it can vary through a small range of values.

Putting these pieces together, let $W_n(\theta, \phi) = aA(\phi)r(\theta)R(\phi)\mathbf{8}(n\theta)$, with $n = 3$ to create the three fold symmetry in Boy's surface. Then

$$B = b + W_3 \tag{1}$$

can be written as

$$B(\theta, \phi) = r(\theta)l(\phi) + aA(\phi)r(\theta)(-\sin 6\theta U(\phi) + 2\sin 3\theta V(\phi)).$$

Both b and W_3 map antipodal points to the same point, so B does as well, thus the image of B is a representation of $\mathbb{R}P^2$ in $\mathbb{R}^3$.

(a) *The Bryant-Kusner Boy's surface.* **(b)** *The Boy's surface constructed in this paper.*

Figure 7: *Top, bottom and side views of Boy's surfaces*

In Figure 7 we see that the Bryant-Kusner Boy's surface [5] and our constructed surface look similar. In fact, horizontal cross sections (on $z = k$) of the image of B are ambient smooth isotopic to the cross sections of the Bryant-Kusner Boy's surface (Figure 8 on the next page, where double points are labelled in red). The image of B near the poles is almost a spherical cap, on which analysis with the key fact $A'(\pm\pi/2) = 0$ shows that $\frac{\partial B}{\partial x}$ and $\frac{\partial B}{\partial y}$ are never zero or colinear. Away from the poles, computer computation verifies that for any a between 0.1 and 0.28, $\frac{\partial B}{\partial \theta}$ and $\frac{\partial B}{\partial \phi}$ are nowhere zero, and the angle between them is never 0 or π. Thus, the image of B is indeed a Boy's surface.

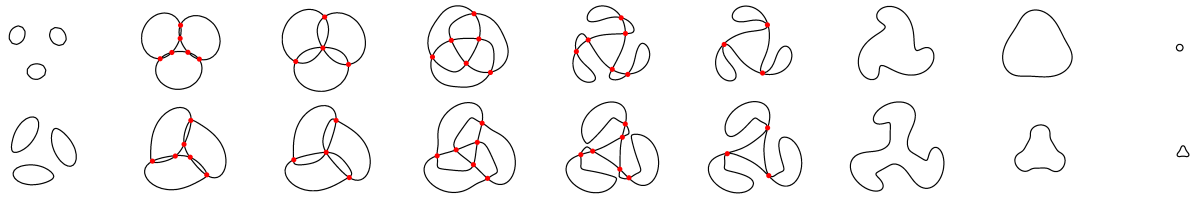

Figure 8: *Cross sections of Boy's surfaces. Top: Bryant-Kusner; Bottom: in this paper.*

Machine

Formula (1) implies that Boy's surface can be drawn by two rotating vectors, added tip to tail. Inspired by this idea, a machine was constructed in which a rigid arm traces the spherical image of b while an attached, rotating screen draws W_3. One can check that

$$B(\theta,\phi) = \langle 0,0,-1/2\rangle + \mathrm{Rot}^z(\theta)\mathrm{Rot}^{-y}(2\phi)[\langle 0,0,1/2\rangle + \mathrm{Rot}^{-x}(\lambda(\phi))aA(\phi)\boldsymbol{\infty}(3\theta)], \tag{2}$$

where $\boldsymbol{\infty}(t) = \langle 0, -2\sin t, \sin 2t\rangle$, and $\mathrm{Rot}^z(\theta)$, $\mathrm{Rot}^{-y}(2\phi)$, and $\mathrm{Rot}^{-x}(\lambda(\phi))$ describe the counter clockwise rotation about the z-axis, and the clockwise rotations about the y and x-axis respectively. Effectively, $l(\phi)$ is $\langle 0,0,1/2\rangle$ rotated by $\mathrm{Rot}^{-y}(2\phi)$ with tail shifted to $\langle 0,0,-1/2\rangle$, and the action of $R(\phi)$ has been decomposed into the actions of $\mathrm{Rot}^{-y}(2\phi)$ and $\mathrm{Rot}^{-x}(\lambda(\phi))$.

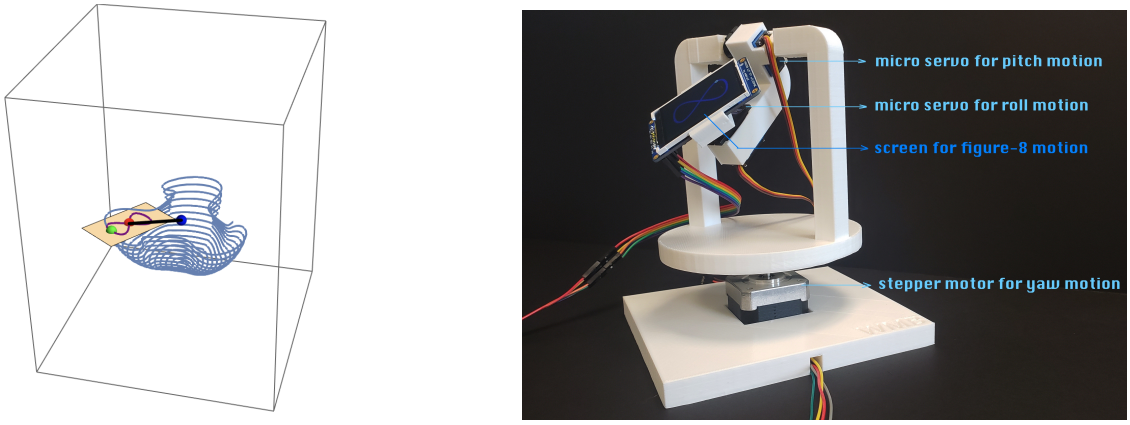

(a) **(b)** *https://www.youtube.com/watch?v=txa7jdZYw7M*

Figure 9: *Conceptual mechanism and practical machine for drawing Boy's surface.*

Formula (2) describes the forward kinematics of an idealized mechanism pictured in Figure 9a. As the robotic "arm" moves about the ball-joint hinged at $(0,0,-\frac{1}{2})$, the screen turns about the axis perpendicular to the arm and lying on the vertical plane, and a single glowing point traces out **8**. Imagine the point as a toy car dashing around this figure-8 track. This was the analogy used in [7].

In the practical design of the machine (Figure 9b), three motors were used to produce the necessary motion: 1) the base stepper generates uniform speed rotation $\mathrm{Rot}^z(\theta)$; 2) the top micro servo controls $\mathrm{Rot}^{-y}(2\phi)$; 3) the bottom micro servo holding the screen controls $\mathrm{Rot}^{-x}(\lambda(\phi))$.

In Figure 9b, electronic and mechanical parts from `Adafruit` are held on a 3D-printed white frame. A single `Arduino Uno` board was sufficient for control and communication, and images were captured using long exposure photography. We programmed the machine to draw the image of B, one parallel at a time. At different ϕ values, the orientation of the screen and the amplitude of the figure-8 differ.

The resulting images for $a \approx 0.13$ are shown in Figure 10 and Figure 11, in which we see that as ϕ gets closer to 0, the image circle eventually folds into a twice traversed trefoil. This trefoil is different from the trefoil curve of self-intersection of the image of b, though they share the triple point at the origin.

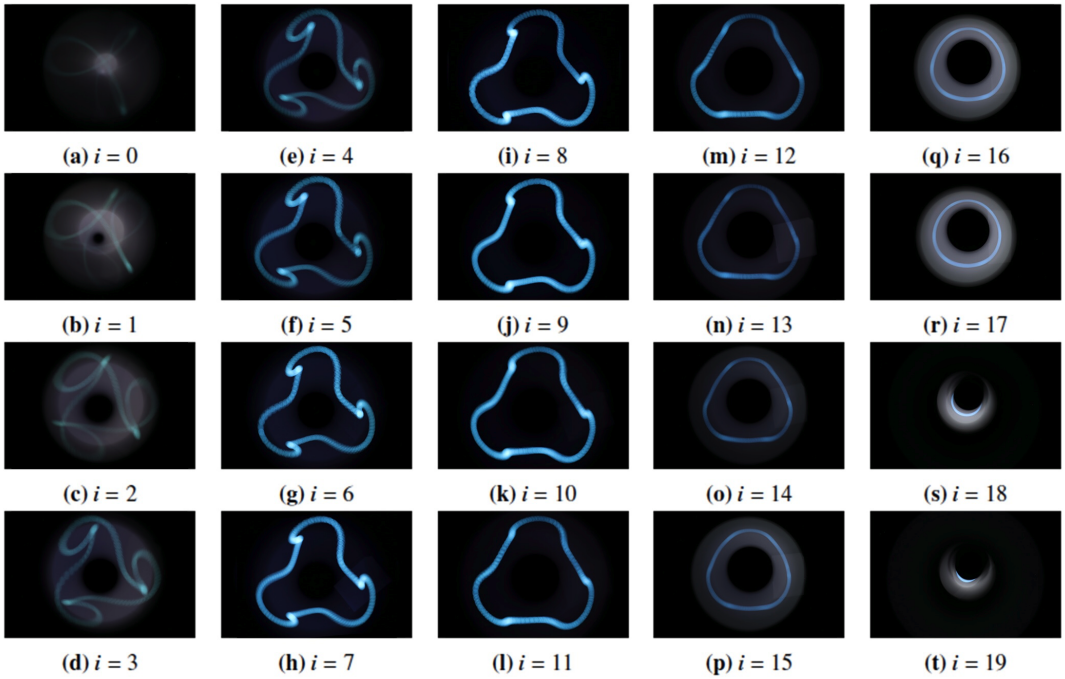

Figure 10: *Top views of images of the parallel* $\phi = \frac{i\pi}{40}$.

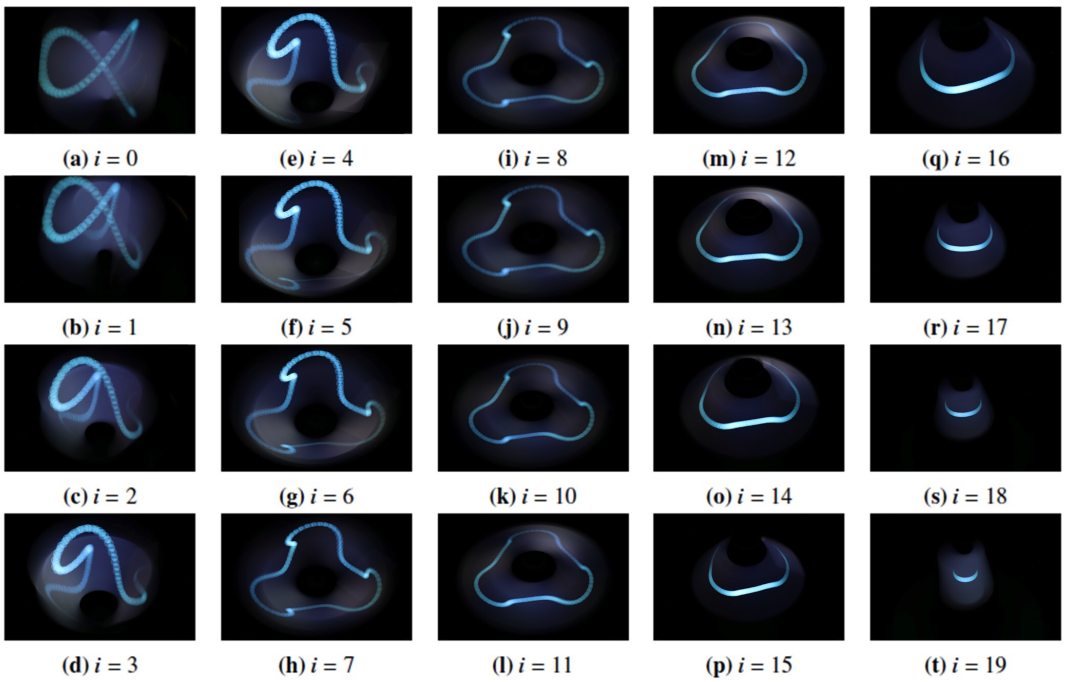

Figure 11: *Side views of images of the parallel* $\phi = \frac{i\pi}{40}$.

Notes

The method we used in this paper can be extended to construct a two-parameter family of immersed $\mathbb{R}P^2$ in $\mathbb{R}^3$. One parameter n (≥ 3) is the period of the waves and the other parameter m is the number of half twists of $R(\phi)$ (following the right hand rule). Both n and m must be odd (and m can be negative) so that antipodal points are identified. The Boy's surface in this paper consists of one half twist ($m = 1$) and period three waves ($n = 3$), thus among these immersions of $\mathbb{R}P^2$, Boy's surface is the simplest. Furthermore, for any m, $\varepsilon - \delta$ proofs can be used to show that there exists an N large enough such that for any $n \geq N$, the surface[2] for m and n is an immersed $\mathbb{R}P^2$.

These immersions can be used as halfway models for sphere eversions [9]. This was the original use of Thurston's corrugation technique. For any given m and sufficiently large n, an analytical formula exists (similar to the one in this paper). Starting with this formula, S^2 can be smoothly deformed into the given immersion of $\mathbb{R}P^2$: the principle meridian regularly deforms to the image of l, such that the north pole remains on the z-axis while the south pole is stationary; meanwhile, the tangent frame of S^2 is twisted into $r(\theta)R(\phi)$ about the tangent vectors of meridians. Since singularities only occur with respect to θ, a single layer of corrugation is sufficient (compare with [3][3]). Once the immersion of $\mathbb{R}P^2$ is reached, we play this movie backward with antipodal points traveling on swapped paths. Thus every point on S^2 trades positions with its antipodal counterpart, and the sphere has been turned inside out. Note that the sphere eversions obtained from different m values can not be deformed into each other. They are like an infinite sequence of adaptations of a movie, with pairwise distinct plot twists.

Acknowledgements

We would like to thank the referees and the program chair David Reimann for helping us improve the presentation of this paper.

References

[1] F. Apéry. *Models of the Real Projective Plane.* Braunschweig; Wiesbaden: Vieweg, 1987.

[2] T. F. Banchoff. "Triple points and surgery of immersed surfaces." *Proc. Amer. Math. Soc.*, Vol. 46, pp 407-413, 1974.

[3] V. Borrelli, S. Jabrane, F. Lazarus, and B. Thibert. "Flat tori in three-dimensional space and convex integration." *Proc. Nat. Acad. Sci. USA*, Vol 109, pp 7218-7223, 2012. https://www.pnas.org/content/109/19/7218

[4] W. Boy. "Über die Curvatura integra und die Topologie geschlossener Flächen." *Math. Ann.*, Vol. 57, pp 151-184, 1903.

[5] H. Karcher and U. Pinkall. "Die Boysche Fläche in Oberwolfach." *Mitteilungen der DMV*, Issue 1, pp 45-47, 1997. https://www.mfo.de/about-the-institute/history/boy-surface/karcher_pinkallboy_surface.pdf

[6] S. Levy, D. Maxwell, T. Munzner, et al. https://youtu.be/OI-To1eUtuU. The Geometry Center, 1994.

[7] S. Levy and W. Thurston. *Making Waves – A Guide to the Ideas behind Outside In.* The Geometry Center, University of Minnesota, 1995. A K Peters/CRC Press, 2009.

[8] H. Samelson. "Shorter Note: Orientibility of Hypersurfaces in $\mathbb{R}^n$." *Proc. Amer. Math. Soc.*, Vol. 22, pp 301-302, 1969.

[9] J. M. Sullivan. http://torus.math.uiuc.edu/jms/Papers/isama/color/opt2.htm. 1999.

[2] We encourage the reader to plot the cross sections of these surfaces. You might be surprised by what you find.

[3] In contrast, infinitely many layers of corrugation have been used to achieve C^1 isometric embeddings.